Impact of arm position on vertebral bone marrow proton density fat fraction in chemical-shift-encoded magnetic resonance imaging: a preliminary study

Tatsuya Hayashi[1]^, Shimpei Yano[2], Shuhei Shibukawa[3,4]^, Shinya Kojima[1]^, Toshimune Ito[1]^, Hiroshi Oba[5], Hiroshi Kondo[5], Asako Yamamoto[5]^, Takahide Okamoto[1]

[1]Graduate School of Medical Technology, Teikyo University, Tokyo, Japan; [2]Central of Radiology, Teikyo University Hospital, Tokyo, Japan; [3]Department of Radiological Technology, Juntendo University, Tokyo, Japan; [4]Center for Evolutionary Cognitive Sciences, Graduate School of Art and Sciences, The University of Tokyo, Tokyo, Japan; [5]Department of Radiology, Teikyo University School of Medicine, Tokyo, Japan

Correspondence to: Tatsuya Hayashi. Graduate School of Medical Technology, Teikyo University, 2-11-1 Kaga, Itabashi-ku, Tokyo 173-8605, Japan. Email: t-hayashi@med.teikyo-u.ac.jp.

Abstract: Arm positions employed during magnetic resonance imaging (MRI) can affect magnetic field distribution, which may result in variability in proton density fat fraction (PDFF) measurements. This study evaluated the effect of arm position on lumbar PDFF measured using chemical-shift-encoded MRI (CSE-MRI). Fifteen healthy volunteers from a single-center underwent lumbar CSE-MRI at two different arm positions (side and elevated) using a single 3T scanner. Scans were performed twice in each position. PDFFs of the L1–L5 vertebrae were independently measured by two readers, and reader measurements were compared by calculating intraclass correlation coefficients (ICC). We compared PDFF measurements from two arm positions and from two consecutive scans using the Wilcoxon test and Bland-Altman analysis. Measurements from the two readers were in high agreement [ICC =0.999; 95% confidence interval (CI), 0.998–0.999]. No significant difference was observed between PDFFs from the first and second scans of all vertebrae for each reader (all P>0.05); however, PDFF for the elevated arm position was significantly higher than that for the side arm position (37.9–44.8% *vs.* 37.0–43.8%; all P<0.05), except at the L2 level by reader 2. The mean differences in PDFF measurements from the first and second scans [0.1%; 95% limits of agreement (LoA), –1.8% to 1.9%] and from the side arm and elevated arm positions (0.8%; 95% LoA, –1.6% to 3.2%) were small. In conclusion, these preliminary data suggest that different arm positions during CSE-MRI can slightly affect lumbar PDFF; however, the mean absolute differences were very small.

Keywords: Bone marrow fat; chemical shift; DIXON; proton density fat fraction (PDFF); magnetic resonance imaging (MRI)

Introduction

Chemical-shift-encoded magnetic resonance imaging (CSE-MRI) is a non-invasive reliable method for quantifying fat content that is widely used for the determination of liver fat or bone marrow fat. The method uses the difference in the chemical shift between water and fat to estimate the signal intensity of the two components and obtain the fat content as the proton density fat fraction (PDFF) (1-4). The

quantitative diagnosis of various pathological conditions has been studied by assessing the PDFF of bone marrow using CSE-MRI. For example, measurement of the PDFF in the lumbar region has been reported to allow for the differentiation between benign and malignant bone marrow lesions (5,6). Other studies have reported changes in the PDFF in vertebral bone marrow caused by osteoporosis (7,8). In addition, the proton density water fraction (100% – PDFF) can be a predictor of bone marrow cellularity, suggesting the possibility of noninvasively assessing bone marrow changes in clinical patients undergoing radiation therapy (9).

The CSE-MRI method has several confounders, such as T1 bias and T2* effect (10,11). As the T1 value of fat is much smaller than that of water, a small flip angle is recommended to minimize any T1 bias. Otherwise, the PDFF will be overestimated due to the faster longitudinal magnetization recovery of fat. Meanwhile, the T2* effect results in the decay of transverse magnetization between echoes, which confounds the PDFF calculation. T2* decay can be compensated for by estimating the T2* using multi-echo acquisition. In addition, the inhomogeneity of the radiofrequency magnetic field (B_1^+) distribution can also affect the PDFF. A change in B_1^+ implies a change in flip angle, thus if the flip angle increases, T1 will be emphasized, leading to a higher measured PDFF due to T1 bias. The B_1^+ distribution is more inhomogeneous at 3T (12). Although this drawback can be improved via the use of dual-source parallel RF excitation (13), the degree of improvement depends on the body region or body habitus. Furthermore, the spatial B_1^+ variability changes the actual flip angles and can affect PDFF measurements (12,14). In fact, in the liver, it has been found that transmit B_1^+ field changes and the PDFF on CSE-MRI can vary depending on the adopted arm position (14). This report indicates the need to consider the preparatory procedures undertaken before performing MRI. In general, a patient's positioning during MRI is dependent on the MRI radiographers. However, both radiologists and MRI radiographers should understand the quantitative effect of changing the patients' arm position. The liver is located in an area spanning from the abdominal side to the dorsal side of the body, whereas the lumbar vertebral bodies are located only on the dorsal side where the B_1^+ is more likely to be obstructed by the arm when the subject is lying with the arms alongside the body. Simply changing the arm position during lumbar vertebral MRI has been reported to improve B_1^+ and signal intensity inhomogeneity (12). However, without proper guidelines,

different MRI radiographers may implement different arm positions to improve the image quality of lumbar MRI. Knowing the effect of these arm-positioning differences during imaging on the measurements will play an important role in their interpretation in future studies. Therefore, we evaluated the effect of arm position on the lumbar PDFF acquired by CSE-MRI.

Methods

Participants

The study was conducted in accordance with the Declaration of Helsinki (as revised in 2013). This study was approved by the Institutional Review Board of Teikyo University (registration No. 21-005), and written informed consent was obtained from all volunteers. The study enrolled 15 healthy volunteers without any spine lesions [12 men and 3 women; average age ± standard deviation (SD) (range), 39.6±11.7 years (22–58 years). Other characteristics [mean ± SD (range)] were as follows: height, 167.7±8.5 cm (145–181 cm); weight, 65.3±12.4 kg (40–88 kg); and body mass index, 21.8±2.7 kg/m² (19.0–30.4 kg/m²).

MRI examination

All scans were performed on a 3T MRI system (MAGNETOM Skyra, Siemens Healthineers, Erlangen, Germany) with a 32-channel spine coil. The "TrueForm" B_1^+ shimming mode was active for the scanner. In this mode, the optimized amplitude and phase transmission settings were used for each region, to minimize B_1^+ inhomogeneity in the subject using a two-channel transmit array. The commercial CSE-MRI sequence made available currently by Siemens Healthineers (q-DIXON) was used in this study. The scan parameters are provided in *Table 1*. A small flip angle and a multi-echo sequence were used to minimize the effect of the T1 bias and T2* decay on the PDFF. CSE-MRI with Controlled Aliasing in Parallel Imaging Results in Higher Acceleration (CAIPIRINHA) (15) was performed over a short scan time within one breath-hold to minimize the effect of respiratory motion. The signal intensities of water and fat corrected for T2* decay were calculated by multi-echo acquisitions and the PDFF map was automatically generated. The subject was placed in a supine position with a cushion under the knees, as in a general lumbar MRI examination. A cushion was also placed above the head, to facilitate arm elevation. To investigate the effect of arm position on the PDFF, all

Table 1 Pulse sequence and imaging parameters

Parameters	MAGNETOM Skyra
Imaging technique	q-DIXON
Pulse sequence	3D GRE
Acquisition matrix	160×160
NSA	1
First TE (ms)	1.18
ΔTE (ms)	1.18
Number of echoes	6
TR (ms)	9.0
Flip angle (°)	4
FOV (mm)	300
Slice thickness (mm)	4.0
Slice spacing (mm)	2.0
Number of slices	40
Acceleration technique	CAIPIRINHA
Acceleration factor	4 (2×2)
Acquisition time (s)	22

NSA, number of signals acquired; TE, echo time; TR, repetition time; FOV, field of view; GRE, gradient echo; CAIPIRINHA, Controlled Aliasing in Parallel Imaging Results in Higher Acceleration.

Side arm position

Elevated arm position

Figure 1 The two different arm positions used during MR scans. This image is published with the participant's consent. MR, magnetic resonance.

volunteers were scanned in two different arm positions (side arm and elevated arm positions) (*Figure 1*). In addition, to confirm the repeatability of the scan itself, two consecutive CSE-MRI scans (first and second scan) were performed in each arm position. First, two consecutive CSE-MRI scans (first and second scan) were performed in the side arm position. Next, the scan table was moved out of the gantry and the position was changed to the elevated arm position, while being careful to change the body position as little as possible. Subsequently, CSE-MRI scans were performed twice in succession in the new position.

PDFF measurements

To assess the inter-reader agreement, the PDFF maps calculated from CSE-MRI were anonymized and regions of interests (ROIs) were drawn on the images independently by two readers, each of whom had more than 10 years of experience in the analysis of MR images. ROIs were placed manually and as large as possible on the five

lumbar vertebral bodies (L1–L5) at the center slice of the lumbar spine on the PDFF map using ImageJ (16,17), so that no obvious artifacts or blood vessels were included (*Figure 2*). The total number of ROIs was 600 (15 cases × 5 vertebral bodies × 2 scans × 2 positions × 2 readers).

Statistical analysis

The degree of agreement between the two readers was evaluated using Bland-Altman analysis and calculating the intraclass correlation coefficient (ICC2, 1) (18). The PDFFs were compared between the first and second scans and between the side and elevated arm positions using the Wilcoxon test and Bland-Altman analysis. In Bland-Altman analysis, the 95% limits of agreement (LoA) was defined as the mean difference $\pm 1.96 \times$ SD. The average of the first and second scans was used for the comparison between the side and elevated arm positions and between the two readers. Significance was set at $P<0.05$. All statistical

5266

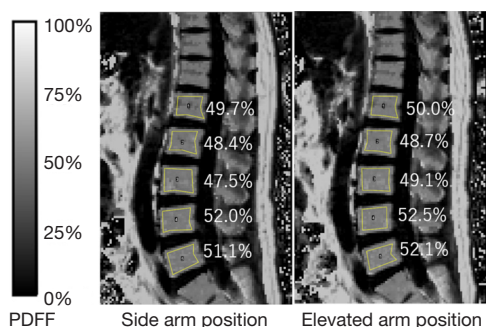Hayashi et al. Impact of arm position on spine PDFF

Figure 2 Location of the ROIs on the PDFF maps. The PDFF can be measured directly by placing the ROI on the PDFF map. PDFF, proton density fat fraction and ROI, region of interest.

analyses were performed using BellCurve for Excel (Social Survey Research Information Co., Ltd., Tokyo, Japan).

Results

Inter-reader agreement

The Bland-Altman plot for the inter-reader agreement is presented in *Figure 3A*. The mean difference (reader 1 – reader 2) was –0.1% [95% confidence interval (CI), –0.2% to 0.03%; 95% LoA, –1.4% to 1.3%]. The PDFF measurements generated by the two readers were highly correlated (ICC =0.999; 95% CI, 0.998 to 0.999).

Differences in PDFF between the first and second scans

The PDFF of each vertebral body is summarized in *Table 2*. There was no significant difference in PDFF between the first and second scans for all vertebral bodies for each reader (all P>0.05). The Bland-Altman plot for the comparison between the first scan and the second scan is shown in *Figure 3B*. The mean difference (first scan – second scan) was 0.1% (95% CI, –0.03% to 0.2%; 95% LoA, –1.8% to 1.9%).

Difference in PDFF between the elevated and side arm positions

The PDFF of each vertebral body is summarized in *Table 3*. The PDFFs obtained in the elevated arm position were significantly higher than those obtained in the side arm position, with the exception of the L2 level for reader 2 (side arm position, 39.1%±15.0% *vs.* elevated arm position, 39.5%±14.8%; P=0.191). The Bland-Altman plot for the comparison between the side arm position and the elevated
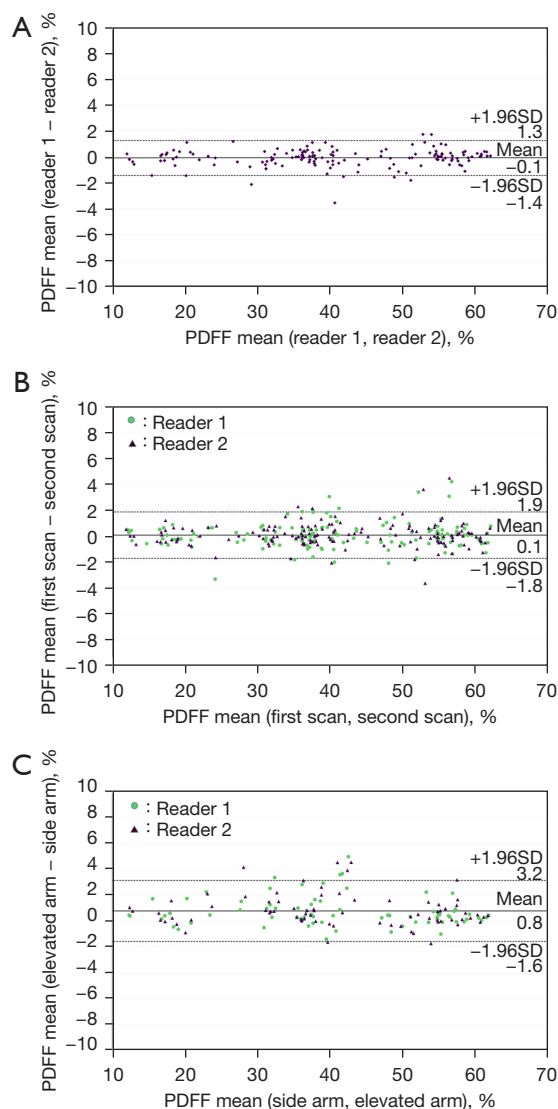

Figure 3 Bland-Altman plots of the differences in PDFF between the two readers (A), between the first and second scans (B), and between the side arm and elevated arm positions (C). The bold line represents the mean difference in the PDFF, and the dashed line represents the range of the 95% LoA (the mean difference ± 1.96 × SD). PDFF, proton density fat fraction; SD, standard deviation; LoA, limits of agreement.

arm position is shown in *Figure 3C*. The mean difference (elevated arm position – side arm position) was 0.8% (95% CI, 0.6% to 1.0%; 95% LoA, –1.6% to 3.2%).

Discussion

The results of the present study show that the PDFF

Table 2 Differences in the PDFF between the first and second scans

Vertebral body	First scan	Second scan	P value
Reader 1			
L1	37.6±14.2	37.3±14.1	0.131
L2	39.2±14.9	39.3±14.8	0.651
L3	41.9±14.0	41.6±13.6	0.804
L4	42.7±13.2	42.8±13.5	0.629
L5	44.0±12.66	44.1±12.7	0.294
Reader 2			
L1	37.8±14.3	37.5±14.2	0.053
L2	39.3±14.6	39.3±14.7	0.558
L3	41.8±13.7	41.5±13.5	0.222
L4	42.7±13.2	42.7±13.4	0.517
L5	44.3±12.8	44.4±12.8	0.206

The first and second scan values include PDFF values for both the side and elevated arm positions. PDFF values (%) are shown as mean ± SD. There was no significant difference in PDFF between the first and second scans for all vertebrae and each reader. PDFF, proton density fat fraction; SD, standard deviation.

Table 3 Differences in the PDFF between the side arm and elevated arm positions

Vertebral body	Side arm position	Elevated arm position	P value
Reader 1			
L1	37.0±14.5	37.9±14.3	0.011*
L2	39.0±15.3	39.5±15.0	0.023*
L3	41.3±14.2	42.2±13.9	0.006*
L4	42.4±13.6	43.1±13.6	0.017*
L5	43.6±12.8	44.5±12.9	0.027*
Reader 2			
L1	37.1±14.6	38.1±14.3	0.003*
L2	39.1±15.0	39.5±14.8	0.191
L3	41.2±13.8	42.2±13.9	0.003*
L4	42.3±13.6	43.1±13.4	0.001*
L5	43.8±13.0	44.8±10.0	0.047*

The side and elevated arm positions include PDFF values for both the first and second scans. PDFF values (%) are shown as mean ± SD. *, significance. PDFF, proton density fat fraction; SD, standard deviation.

measurements obtained by CSE-MRI using the elevated arm position were slightly but significantly higher than those in the side arm position. The variability in PDFF according to arm position was higher than that caused by the CSE-MRI sequence itself and inter-reader differences. Even if the B_1^+ shimming system is adopted, B_1^+ variation caused by arm position occurs in the lumbar spine. To the best of our knowledge, lumbar spine MRI is usually performed in the side arm position; however, raising or slightly lifting the arm has been reported to improve B_1^+ inhomogeneity, thus improving diagnostic image quality (12). Therefore, in the absence of specific guidelines regarding a patient's arm position during lumbar spine MRI, different MRI radiographers may implement different arm positions to improve image quality. Prior to this study, the influence of arm position on PDFF measurements had not been systematically studied. The results of this study showed that the effect of arm positioning was significant but very small. This suggests that there is a degree of flexibility in arm positioning that allows MRI radiographers to prioritize a patient's condition or image quality, without significantly impacting PDFF measurements. Additionally, in light of the findings of the present study and that by Ishizaka *et al.* (12), we recommend that slightly lifted arms should be used as

the default position in spine examinations using MRI, as it improves morphological images while having a negligible impact on PDFF. However, the position of the patient may be changed depending on their condition or habitus.

From the lumbar spine to the sacrum, B_1^+ is disturbed when the arm is placed in the side position, indicating that the actual flip angle is lower than the set flip angle (12). Because of the difference in T1 between water and fat (T1 bias), the degree of T1 weighting is affected by changes in the flip angle, resulting in changes in the PDFF. The increase in PDFF observed in the elevated arm position compared with the side arm position can be attributed to the increase in the flip angle as a result of the improvement in B_1^+ inhomogeneity. Conversely, this is not necessarily the case in the liver region (14). Although differences in arm positioning during MRI of the liver region have been reported to alter B_1^+ distribution and, thus, affect PDFF, the variability of B_1^+ associated to arm positioning depends on the segment of the liver; i.e., the PDFF may increase or decrease depending on arm position. This is because the liver has a complex shape and is located in an area spanning from the anterior to the posterior side of the abdomen; thus, the distortion of B_1^+ varies according to the liver segment. For example, the lateral segment showed an

improvement in B_1^+, whereas the medial anterior posterior segment showed a decrease in B_1^+ (14). Therefore, elevation of the arms tended to increase the PDFF in the lumbar spine, whereas this is not necessarily the case in the liver.

We must consider whether the changes in PDFF observed in the current study have any clinical significance. Schmeel *et al.* reported that the PDFF of malignant vertebral compression fractures is significantly lower than that of acute benign vertebral compression fractures, with a high diagnostic performance in differentiating those fractures (PDFF, 3.48%±3.30% *vs.* 23.99%±11.86%; area under the curve, 0.98) (6). In addition, Yoo *et al.* showed that PDFF maps created using CSE-MRI can be useful to distinguish between benign and malignant causes of local bone marrow abnormalities in cases in which qualitative diagnosis using conventional MR images is difficult (5). The PDFF of malignant focal bone lesions was significantly lower than that of other focal benign lesions, including Modic type 1 changes, Schmorl's nodes, focal red-marrow, and benign fracture (2.8%±3.1% *vs.* 16.5%±14.0%) (5). Furthermore, Gassert *et al.* found that the PDFF, as a potential biomarker of bone fragility, can distinguish between osteoporotic or osteopenic patients with and without vertebral fractures; in patients with osteoporosis/osteopenia, the mean PDFF was significantly higher in those with vertebral fractures compared with those without vertebral fractures (61.1%±10.1% *vs.* 39.2%±11.2%) (8). Because the differences in PDFF obtained from the comparisons performed in those reports are much larger than the changes observed in the present study, the effect of arm position during CSE-MRI on lesion differentiation is considered to be negligibly small.

The inter-reader agreement of the current study was excellent (ICC =0.999). Moreover, the difference in PDFF between two consecutive scans was small (mean difference, 0.1%; 95% LoA, −1.8% to 1.9%). Therefore, the variability of the PDFF caused by the change in arm positioning does not seem to be dependent on the CSE-MRI sequence itself or on the reader. In a multi-vendor, multi-center study, the inter-reader absolute agreement among PDFF measurements from three imagers and two reader combinations was also excellent (ICC =0.986), and the mean differences in PDFF reported across various MR machines from two different vendors (GE Healthcare and Philips Healthcare) and at two field strengths (1.5T and 3.0T) ranged from 0.6% to 1.5%, with a 95% LoA within ±3.4% (19). The variation of the PDFF according to the arm positions (mean difference, 0.8%; 95% LoA, −1.6% to

3.2%) appears to be comparable to that detected between vendors. Although this variability is small and may have no clinical significance, it should be noted that raising the arm slightly increases the PDFF; therefore, follow-up PDFF measurements should be performed using the same arm position.

The PDFF measurements obtained in this study tended to increase from L1 to L5, which is consistent with the results of previous studies (7,20,21). A possible reason for this increase is the age-related change from red marrow to yellow marrow from L5 to L1; however, the pathophysiological relationship has not been fully investigated (20,21).

This study has several limitations. First, the study was performed using a single scanner at a single institution. Because the specifications of the B_1^+ shimming system vary from vendor to vendor, a study involving multiple vendors and institutions is desirable to obtain additional data. Second, our sample size was small, thus the data generated can be considered as preliminary data. Our priority in this study was to clarify whether the position of the arm during CSE-MRI has an impact on PDFF measurements. Therefore, it was sufficient to confirm the relationship between PDFF measurements and arm positioning. Larger cohorts will be needed to further elucidate the impact of this small change.

Although preliminary, the results of this study suggest that different arm positions during CSE-MRI can slightly affect lumbar PDFF values; however, the mean absolute differences were very small. Given the small impact of arm position on PDFF, MRI radiographers may choose to prioritize the patient's condition or image quality when performing CSE-MRI.

Acknowledgments

Footnote

Conflicts of Interest: All authors have completed the ICMJE uniform disclosure form (available at https://qims.amegroups.com/article/view/10.21037/qims-22-396/coif). The authors have no conflicts of interest to declare.

Ethical Statement: The authors are accountable for all

aspects of the work in ensuring that questions related to the accuracy or integrity of any part of the work are appropriately investigated and resolved. The study was conducted in accordance with the Declaration of Helsinki (as revised in 2013). The study was approved by the Institutional Review Board of Teikyo University (registration No. 21-005), and informed consent was obtained from all individual participants.

Open Access Statement: This is an Open Access article distributed in accordance with the Creative Commons Attribution-NonCommercial-NoDerivs 4.0 International License (CC BY-NC-ND 4.0), which permits the non-commercial replication and distribution of the article with the strict proviso that no changes or edits are made and the original work is properly cited (including links to both the formal publication through the relevant DOI and the license). See: https://creativecommons.org/licenses/by-nc-nd/4.0/.

References

1. Karampinos DC, Ruschke S, Dieckmeyer M, Diefenbach M, Franz D, Gersing AS, Krug R, Baum T. Quantitative MRI and spectroscopy of bone marrow. J Magn Reson Imaging 2018;47:332-53.
2. Kim HJ, Cho HJ, Kim B, You MW, Lee JH, Huh J, Kim JK. Accuracy and precision of proton density fat fraction measurement across field strengths and scan intervals: A phantom and human study. J Magn Reson Imaging 2019;50:305-14.
3. Hu HH, Yokoo T, Bashir MR, Sirlin CB, Hernando D, Malyarenko D, et al. Linearity and Bias of Proton Density Fat Fraction as a Quantitative Imaging Biomarker: A Multicenter, Multiplatform, Multivendor Phantom Study. Radiology 2021;298:640-51.
4. Sollmann N, Löffler MT, Kronthaler S, Böhm C, Dieckmeyer M, Ruschke S, Kirschke JS, Carballido-Gamio J, Karampinos DC, Krug R, Baum T. MRI-Based Quantitative Osteoporosis Imaging at the Spine and Femur. J Magn Reson Imaging 2021;54:12-35.
5. Yoo HJ, Hong SH, Kim DH, Choi JY, Chae HD, Jeong BM, Ahn JM, Kang HS. Measurement of fat content in vertebral marrow using a modified dixon sequence to differentiate benign from malignant processes. J Magn Reson Imaging 2017;45:1534-44.
6. Schmeel FC, Luetkens JA, Enkirch SJ, Feißt A, Endler CH, Schmeel LC, Wagenhäuser PJ, Träber F, Schild HH, Kukuk GM. Proton density fat fraction (PDFF) MR imaging for differentiation of acute benign and neoplastic compression fractures of the spine. Eur Radiol 2018;28:5001-9.
7. Li X, Xie Y, Lu R, Zhang Y, Li Q, Kober T, Hilbert T, Tao H, Chen S. Q-Dixon and GRAPPATINI T2 Mapping Parameters: A Whole Spinal Assessment of the Relationship Between Osteoporosis and Intervertebral Disc Degeneration. J Magn Reson Imaging 2022;55:1536-46.
8. Gassert FT, Kufner A, Gassert FG, Leonhardt Y, Kronthaler S, Schwaiger BJ, Boehm C, Makowski MR, Kirschke JS, Baum T, Karampinos DC, Gersing AS. MR-based proton density fat fraction (PDFF) of the vertebral bone marrow differentiates between patients with and without osteoporotic vertebral fractures. Osteoporos Int 2022;33:487-96.
9. MacEwan IJ, Glembotski NE, D'Lima D, Bae W, Masuda K, Rashidi HH, Mell LK, Bydder M. Proton density water fraction as a biomarker of bone marrow cellularity: validation in ex vivo spine specimens. Magn Reson Imaging 2014;32:1097-101.
10. Liu CY, McKenzie CA, Yu H, Brittain JH, Reeder SB. Fat quantification with IDEAL gradient echo imaging: correction of bias from T(1) and noise. Magn Reson Med 2007;58:354-64.
11. Hines CD, Yu H, Shimakawa A, McKenzie CA, Brittain JH, Reeder SB. T1 independent, T2* corrected MRI with accurate spectral modeling for quantification of fat: validation in a fat-water-SPIO phantom. J Magn Reson Imaging 2009;30:1215-22.
12. Ishizaka K, Kudo K, Harada K, Shirai T, Fujiwara T, Aoike S, Takamori S, Shirato H. Simple modification of arm position improves B1+ and signal homogeneity in the thoracolumbar spine at 3T. J Magn Reson Imaging 2018;47:123-30.
13. Bouvier J, Troprès I, Lamalle L, Grand S, Breil S, Le Bas JF, Krainik A. Evaluation of dual-source parallel RF excitation technology in MRI of thoraco-lumbar spine at 3.0 T. J Neuroradiol 2013;40:94-100.
14. Watanabe S, Shibukawa S, Hayashi T, Tsuruya K, Niwa T. Influence of arm position on proton density fat fraction in the liver using chemical shift-encoded magnetic resonance imaging. Magn Reson Imaging 2021;83:133-8.
15. Breuer FA, Blaimer M, Heidemann RM, Mueller MF, Griswold MA, Jakob PM. Controlled aliasing in parallel imaging results in higher acceleration (CAIPIRINHA) for multi-slice imaging. Magn Reson Med 2005;53:684-91.
16. Le Ster C, Gambarota G, Lasbleiz J, Guillin R, Decaux

5270

Hayashi et al. Impact of arm position on spine PDFF

O, Saint-Jalmes H. Breath-hold MR measurements of fat fraction, T1, and T2 * of water and fat in vertebral bone marrow. J Magn Reson Imaging 2016;44:549-55.

17. Abramoff MD, Magelhaes PJ, Ram SJ. Image Processing with ImageJ. Biophotonics International 2004;11:36-42.

18. Koo TK, Li MY. A Guideline of Selecting and Reporting Intraclass Correlation Coefficients for Reliability Research. J Chiropr Med 2016;15:155-63.

19. Schmeel FC, Vomweg T, Träber F, Gerhards A, Enkirch SJ, Faron A, Sprinkart AM, Schmeel LC, Luetkens JA, Thomas D, Kukuk GM. Proton density fat fraction MRI of vertebral bone marrow: Accuracy, repeatability, and reproducibility among readers, field strengths, and imaging platforms. J Magn Reson Imaging 2019;50:1762-72.

20. Li GW, Xu Z, Chen QW, Tian YN, Wang XY, Zhou L, Chang SX. Quantitative evaluation of vertebral marrow adipose tissue in postmenopausal female using MRI chemical shift-based water-fat separation. Clin Radiol 2014;69:254-62.

21. Baum T, Yap SP, Dieckmeyer M, Ruschke S, Eggers H, Kooijman H, Rummeny EJ, Bauer JS, Karampinos DC. Assessment of whole spine vertebral bone marrow fat using chemical shift-encoding based water-fat MRI. J Magn Reson Imaging 2015;42:1018-23.